

Model for cardiorespiratory synchronization in humans

Kiyoshi Kotani,¹ Kiyoshi Takamasu,¹ Yosef Ashkenazy,² H. Eugene Stanley,² and Yoshiharu Yamamoto^{3,*}
¹*Department of Precision Engineering, Graduate School of Engineering, The University of Tokyo, 7-3-1 Hongo, Bunkyo-ku, Tokyo 113-8656, Japan*

²*Center for Polymer Studies and Department of Physics, Boston University, Boston, Massachusetts 02215*

³*Educational Physiology Laboratory, Graduate School of Education, University of Tokyo, Tokyo 113-0033, Japan*

(Received 20 November 2001; published 21 May 2002)

Recent experimental studies suggest that there is evidence for a synchronization between human heartbeat and respiration. We develop a physiologically plausible model for this cardiorespiratory synchronization, and numerically show that the model can exhibit stable synchronization against given perturbations. In our model, in addition to the well-known influence of respiration on heartbeat, the influence of heartbeat (and hence blood pressure) on respiration is also important for cardiorespiratory synchronization.

DOI: 10.1103/PhysRevE.65.051923

PACS number(s): 87.19.Hh, 87.80.Vt, 05.45.Xt

I. INTRODUCTION

Synchronization is a general phenomenon that plays an important role in biological and physiological systems [1,2]. For a dual oscillator system, synchronization is defined [3] by

$$|n\phi_1 - m\phi_2| < \epsilon, \quad (1)$$

where n and m are integers that describe the ratio of the synchronized oscillations, $\phi_{1,2}$ are phases of the oscillators, and ϵ is a small positive constant.

Recent studies have focused on the synchronization between two vital oscillators in humans, heartbeat and respiration. Schäfer and co-workers [4–6] recorded resting human heartbeats (R waves of an electrocardiogram) and respiration for 30 min, and plotted instantaneous respiratory phases at each occurrence of heartbeat against the beat number. They found horizontally striped plots for some subjects, indicating that relation (1) is satisfied for sufficiently long periods of time. They also showed that the degree of synchronization is inversely proportional to the magnitude of the respiratory modulation of cardiac cycle lengths [4], known as respiratory sinus arrhythmia (RSA), and concluded that there are two competing factors in cardiorespiratory interactions. Furthermore, Seidel and Herzel [7] reported similar synchronization behavior for 213 cardiac cycles in their experiment. They compared the beat number per single breath of original data with that of stochastic surrogate data, and found the probability that the observed synchronization was due to a chance event was extremely low ($\approx 3 \times 10^{-4}$).

A general understanding of the mechanisms of synchronization behavior is lacking. Further experimental investigations in humans might shed light, but human physiological experiments are associated with problems such as the limited length of data and intrinsic nonstationarity. Instead, we develop a physiologically plausible structural model, that can simulate cardiorespiratory synchronization. Such a model, if successfully developed, would be useful in investigating

conditions under which cardiorespiratory synchronization is observed, and hence designing further experimental as well as theoretical studies of this phenomenon.

Structural cardiovascular and/or cardiorespiratory modeling has a long history. One of the most famous models is the one proposed by DeBoer *et al.* [8]. This is a simple beat-to-beat model describing relationships among blood pressures, respiration, peripheral resistance, and cardiac interbeat intervals. This model has further been elaborated recently by Seidel and Herzel [9] (SH) to take into account detailed factors such as the sinus node responsiveness, autonomic neurotransmitter kinetics, and time-dependent (Windkessel) vascular dynamics. SH also incorporated into their model physiologically plausible nonlinear interactions that were found to generate even chaotic dynamics. However, the models of both DeBoer *et al.* and SH only considered respiratory influences on heartbeat, not the opposite effect where the heartbeat affects respiration. In other words, there is no mutual interaction between these two oscillators in their models, which sometimes exists in models showing synchronization phenomena [1,10,11]. Thus, in the present study, we add to the SH model an effect of heartbeat and the resultant changes in the baroreceptor afferent activity, which is known to be present in physiology experiments [12,13], and found that this modification results in the cardiorespiratory synchronization.

This paper is organized as follows. In Sec. II, we describe the cardiovascular model emphasizing the key difference from the SH model, namely, the additional effect of heartbeat on respiration. Section III contains results of numerical simulations and consideration of the parameter region where the cardiorespiratory synchronization in this model is observed and the stability of the synchronization. We also study effects of noise on synchronization. In Sec. IV, we provide a mechanism accounting in part for the results in our model. Finally, in Sec. V, we summarize our results and discuss some implications of our model for future research on “complex” cardiovascular dynamics in humans.

II. METHODS

A. Model description

Figure 1 schematically describes the model used in the present study. The original SH model consists of (i) neural

*Electronic address: yamamoto@p.u-tokyo.ac.jp

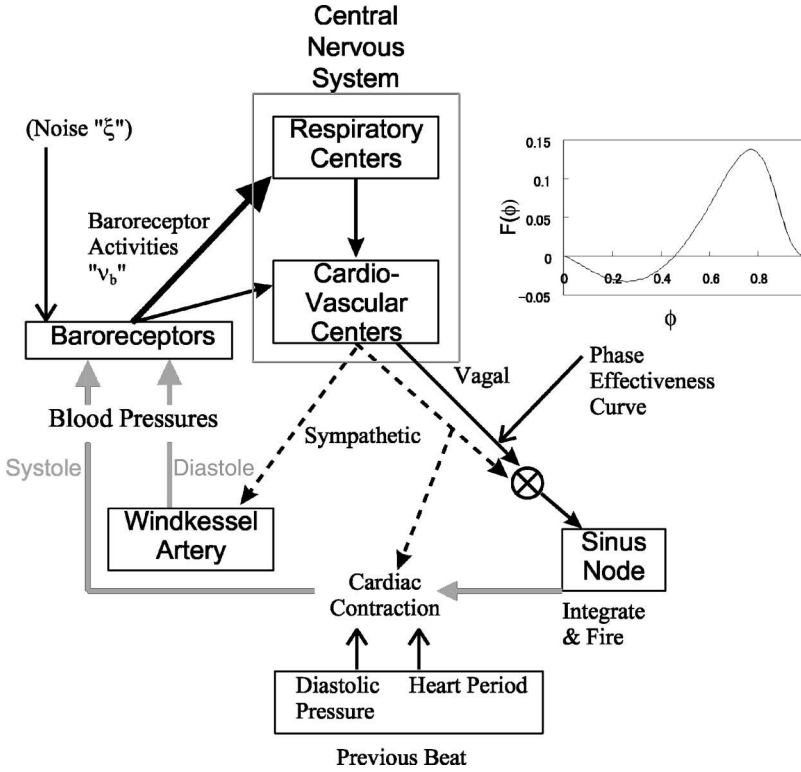


FIG. 1. Schematic diagram of the cardiovascular model in this study. The effects of baroreflex to the respiratory phase are newly added to the original SH model [9]. In the simulations with noise, the noise was injected to ν_b , i.e., the baroreceptor afferents. The diversity of this model is caused mainly by factors such as time delays in the neural conduction, phase effectiveness of the sinus node, multiplications in neural and mechanical variables, and time-varying Windkessel dynamics.

afferents from baroreceptors to the central nervous system, (ii) autonomic (vagal and sympathetic) neural efferents from the brain stem cardiovascular centers, and (iii) mechanical signal transductions within the cardiovascular system finally setting the arterial blood pressures.

In this model, the baroreceptor activity ν_b is first set by blood pressure p (mmHg; 0.133 kPa) and its first derivative as

$$\nu_b = k_1(p - p^{(0)}) + k_2 \frac{dp}{dt}, \quad (2)$$

where $k_1 = 0.02 \text{ mmHg}^{-1}$, $k_2 = 0.00125 \text{ s mmHg}^{-1}$, and $p^{(0)} = 50.0 \text{ mmHg}$. This ν_b subsequently determines the efferent sympathetic (ν_s) and vagal or parasympathetic (ν_p) activities, after being modulated by respiratory influence R , as

$$\nu_s = \max[0, \nu_s^{(0)} - k_s^b \nu_b + k_s^r(1 - R)], \quad (3)$$

where $\nu_s^{(0)} = 0.8$, $k_s^b = 0.7$, and $k_s^r = 0.035$ and

$$\nu_p = \max[0, \nu_p^{(0)} + k_p^b \nu_b + k_p^r(1 - R)], \quad (4)$$

where $\nu_p^{(0)} = 0.0$, $k_p^b = 0.3$, and $k_p^r = 0.035$. In the original SH model, the respiratory influence on the autonomic neural efferents was a rectified sinusoidal wave with fixed frequency (0.2 Hz) and phase (0.0 rad). However, our model incorporates the dependency of R upon ν_b and hence on a momentary blood pressure level (see below).

Next, the heartbeat is generated by an integrate-and-fire model when the pacemaker phase (ϕ) of the sinus node hits the threshold of 1.0: ϕ is reset to zero immediately after the

firing. The phase velocity is a function of both sympathetic (f_s) and parasympathetic (f_p) influences on the sinus node,

$$\frac{d\phi}{dt} = \frac{1}{T^{(0)}} f_s f_p, \quad (5)$$

where $T^{(0)} = 1.1 \text{ s}$, and the sympathetic influence f_s (facilitatory) is a function of cardiac concentration (c_{cNe}) of sympathetic neurotransmitter “norepinephrine” (Ne),

$$f_s = 1 + k_\phi^{cNe} \left[c_{cNe} + (\hat{c}_{cNe} - c_{cNe}) \frac{(c_{cNe})^{n_{cNe}}}{(\hat{c}_{cNe})^{n_{cNe}} + (c_{cNe})^{n_{cNe}}} \right], \quad (6)$$

where $k_\phi^{cNe} = 1.6$, $\hat{c}_{cNe} = 2.0$, and $n_{cNe} = 2.0$. As the release of Ne by the neural input ν_s is known to have a slow kinetics, the c_{cNe} kinetics is described, after incorporating the neural conduction delay ($\theta_{cNe} = 1.65 \text{ s}$), by the first-order model,

$$\frac{dc_{cNe}}{dt} = -\frac{c_{cNe}}{\tau_{cNe}} + k_{cNe}^s \nu_s(t - \theta_{cNe}), \quad (7)$$

where $\tau_{cNe} = 2.0 \text{ s}$ and $k_{cNe}^s = 1.2$.

The parasympathetic influence f_p (inhibitory) assumes no transmitter kinetics, because the kinetics of neurotransmitter “acetylcholine” is sufficiently fast, and the f_p is a direct function of the neural input ν_p . However, based on experimental findings that the vagal stimulation had greater bradycardic effects especially in the latter half of cardiac cycles [14], the phase effectiveness curve $F(\phi)$ is incorporated. Thus,

$$f_p = 1 - k_\phi^p \left[\nu_p(t - \theta_p) + [\hat{\nu}_p - \nu_p(t - \theta_p)] \right. \\ \left. \times \frac{\nu_p(t - \theta_p)^{n_p}}{\hat{\nu}_p^{n_p} + \nu_p(t - \theta_p)^{n_p}} \right] F(\phi), \quad (8)$$

where $\theta_p = 0.5$ s, $k_\phi^p = 5.8$, $\hat{\nu}_p = 2.5$, $n_p = 2.0$, and

$$F(\phi) = \phi^{1.3} (\phi - 0.45) \frac{(1 - \phi)^3}{(1 - 0.8)^3 + (1 - \phi)^3}. \quad (9)$$

The systolic part of blood pressure is determined by diastolic pressure of the previous beat d_{i-1} (mmHg) and cardiac contractility of the current beat S_i ,

$$p = d_{i-1} + S_i \frac{t - t_i}{\tau_{sys}} \exp\left(1 - \frac{t - t_i}{\tau_{sys}}\right), \quad (10)$$

where t_i is the time of last contraction onset and $\tau_{sys} = 0.125$ s. The S_i is a function of the duration of previous heart period T_i (s) through the Frank-Starling mechanism (i.e., the greater cardiac filling results in the greater contractility), as well as the cardiac concentration of Ne [Eq. (7)]. This is described by

$$S_i' = S^{(0)} + k_S^c c_{cNe} + k_S^t T_{i-1}, \quad (11)$$

where $S^{(0)} = 25$ mmHg, $k_S^c = 40$ mmHg, and $k_S^t = 10$ mmHg s⁻¹ and

$$S_i = S_i' + (\hat{S} - S_i') \frac{S_i'^{n_S}}{S_i'^{n_S} + \hat{S}^{n_S}}, \quad (12)$$

where $\hat{S} = 70$ mmHg and $n_S = 2.5$.

The diastolic part of blood pressure is described by the relaxation of the Windkessel arteries with a time-varying relaxation “constant” τ_v (s),

$$\frac{dp}{dt} = -\frac{p}{\tau_v(t)}, \quad (13)$$

and the τ_v is a function of vascular concentration of Ne (c_{vNe}) as

$$\tau_v = \tau_v^{(0)} - \bar{\tau}_v \left[c_{vNe} + (\hat{c}_{vNe} - c_{vNe}) \frac{c_{vNe}^{n_{vNe}}}{c_{vNe}^{n_{vNe}} + \hat{c}_{vNe}^{n_{vNe}}} \right], \quad (14)$$

where $\tau_v^{(0)} = 2.2$ s, $\bar{\tau}_v = 1.2$ s, $\hat{c}_{vNe} = 10.0$, and $n_{vNe} = 1.5$. Like Eq. (7), the c_{vNe} has first-order kinetics with the conduction delay θ_{vNe} (s),

$$\frac{dc_{vNe}}{dt} = -\frac{c_{vNe}}{\tau_{vNe}} + k_{c_{vNe}}^s \nu_s(t - \theta_{vNe}), \quad (15)$$

where $\tau_{vNe} = 2.0$ s and $k_{c_{vNe}}^s = 1.2$. According to Seidel and Herzl [9], an increase in the vascular sympathetic delay θ_{vNe} to 4.2 s leads via a Hopf bifurcation to low-frequency

(≈ 0.1 Hz), sustained heart rate oscillations [Mayer wave sinus arrhythmia (MWSA)] frequently observed in human experiments [15,16]. Thus, we adopt this value as θ_{vNe} in the present study.

As shown above, it is apparent that the original SH model only considers unidirectional, respiratory influences on heartbeat, not the opposite effect where the heartbeat affects respiration. We hypothesize that a mutual interaction between respiration and heartbeat might be essential for the cardiorespiratory synchronization because such an effect sometimes exists in models showing synchronization phenomena [1,10,11]. Indeed, previous experimental results showed that, while baroreceptor stimuli did not affect the tidal ventilatory volume, they did lengthen the period of expiration in anesthetized dogs [12,13].

To incorporate this factor, we first introduce an instantaneous phase of respiration r , where $0.0 < r \leq 0.5$ and $0.5 < r \leq 1.0$, respectively, correspond to expiratory and inspiratory periods. With this r , the respiratory influences R in Eqs. (3) and (4) are described by

$$R = \cos(2\pi r). \quad (16)$$

Without the influence of baroreceptor afferents, the r has a constant phase velocity of

$$\frac{dr}{dt} = \frac{1}{T_{resp}}, \quad (17)$$

where T_{resp} is a constant respiratory period.

Then we add the effect of the baroreceptor afferents on the respiratory phase: if $\nu_b > \nu_{trig}$ during expiration [$\sin(2\pi r) > 0.0$], then r is modulated as

$$\frac{dr}{dt} = \frac{1}{T_{resp}} - G(\nu_b - \nu_{trig}), \quad (18)$$

where T_{resp} is a constant respiratory period and G and $\nu_{trig} = 1.3$ are constant values. Note that the higher ν_b results in the slower phase velocity during expiration, and thus lengthens the period of expiration as observed in the experimental studies [12,13].

B. Data analysis

A set of delay-differential equations above was numerically integrated by a Runge-Kutta method of fourth order with a constant step size (5 ms). To handle the time delays in Eqs. (7), (8), and (15), we used ring buffers for sympathetic and vagal activities, which store their immediate history. In all simulations, we skipped first 180 s to exclude transients, and recorded the following 5000 s.

Before evaluating the cardiorespiratory synchronization in our model, we tuned two parameters, k_s^r in Eq. (3) and k_p^r in Eq. (4), so that the magnitudes of both RSA and MWSA were comparable with those typically observed in human experiments. To achieve this, we ran simulations with $T_{resp} = 4.5$ s and $G = 0.0$ in Eq. (18), calculated the spectral powers for both RSA and MWSA, and compared the results with those obtained in an experiment [17] with the same (in terms

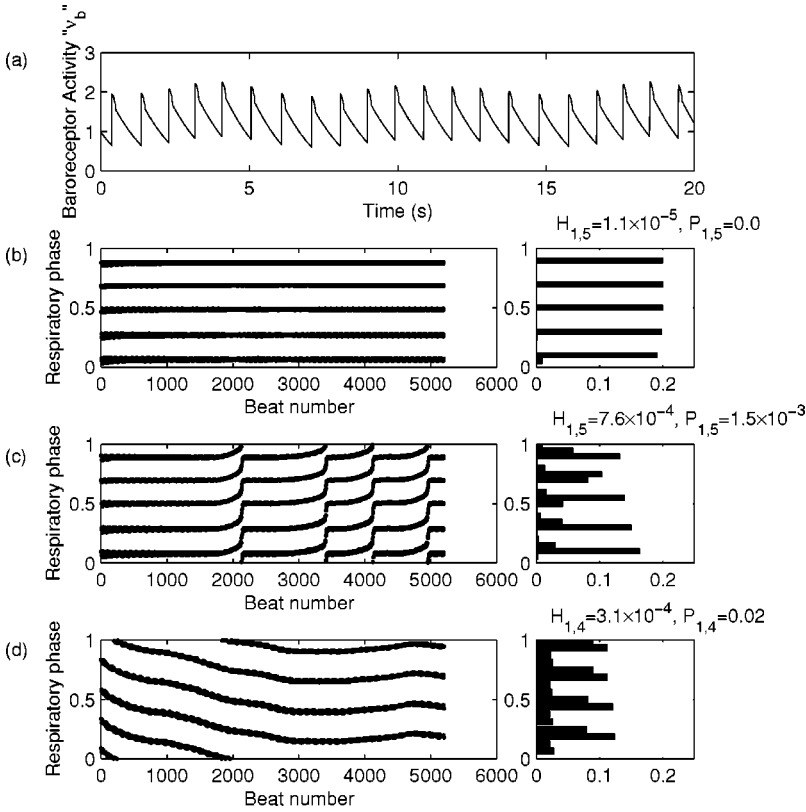


FIG. 2. Representative results of simulations without noise and the corresponding values for H and P . (a) Baroreceptor activity ν_b . (b) The phase stroboscope (a diagram for the instantaneous respiratory phase at each heartbeat; left) and the histogram of the instantaneous phases (right) with $(G, T_{resp}) = (0.2, 4.52)$. The H and P are small enough to be judged for the stable synchronization. (c) The phase stroboscope and the histogram with $(G, T_{resp}) = (0.2, 4.48)$. This is an example of phase locking without frequency locking. (d) The phase stroboscope and the histogram with $(G, T_{resp}) = (2.8 \times 10^{-2}, 4.90)$. This is an example of frequency locking without phase locking.

of T_{resp}) condition. The parameter values of $k_s^r = k_p^r = 0.035$, and the initial values of $p = 110.0$ mmHg, $c_{cNe} = c_{vNe} = 0.15$, $d_0 = 90.0$ mmHg, $S_0 = 40.0$ mmHg, and $T_0 = 1.10$ s were determined so that the simulated RSA and MWSA as well as the mean heartbeat interval were all within one standard deviation of the experimental values [18].

Synchronization is classified into three types [6,19]: (i) frequency and phase lockings, (ii) a phase locking without a frequency locking, and (iii) a frequency locking without a phase locking among multiple oscillators. In this paper, we defined the cardiorespiratory synchronization only in the first sense continuing for the entire period of simulation (5000 s), and introduced the following two criteria to judge whether the synchronization was observed in our model.

First, we define an index of frequency locking as

$$H_{m,n} \equiv \left| \sum_{i=n+1}^L \frac{1}{2\pi m(L-n)} (\Phi_i - \Phi_{i-n} - 2\pi m) \right|, \quad (19)$$

where L is the total number of beats, Φ_i is an instantaneous respiratory phase when the i th heartbeat occurs, $m = 1, 2, 3$, and $n = 1, 2, 3, \dots$. This $H_{m,n}$ indicates how much the respiratory phase slips during the entire course of simulation as compared to a complete $m:n$ frequency locking. Hence, $H_{m,n} = 0.0$ if there is a complete $m:n$ frequency locking, and $H_{m,n}$ increases as the locking becomes weak [e.g., see Figs. 2(b–d)].

Under the frequency locked condition, the data array $\Phi_i \bmod 2\pi$ ($i = 1, 2, 3, \dots, L$) was divided into $4n$ parts because the phase slips every $2\pi/n$. Then, an index of phase locking $P_{m,n}$ was calculated as the minimal probability dis-

tribution of such a histogram by dividing the minimal phase distribution by the total number of beats. The $P_{m,n}$ also has the minimal value of 0.0, and increases as the locking becomes weak [e.g., see Figs. 2(b–d)].

III. RESULTS

A. Synchronization without noise

To judge whether we could obtain the stable synchronization behavior in our model, we set the criteria of $H_{m,n} < 5.0 \times 10^{-4}$ and $P_{m,n} < 0.002$. This we did by visual inspection of multiple phase “stroboscopes” so that we could discriminate a pattern associated with both frequency and phase lockings from others.

Figure 2 shows examples for simulations without injecting noise into the baroreceptor activity (see following section for the results with noise). When $(G, T_{resp}) = (0.2, 4.52)$, the phase stroboscope [Fig. 2(b), left], i.e., an instantaneous respiratory phase at each heartbeat, showed a perfect 1:5 synchronization also resulting in five sharp peaks in the histogram [Fig. 2(b), right]. The index $H_{1,5}$ was sufficiently small and we could confirm the acceptable frequency locking. Also, as the histogram contained many bins without distributions, the index $P_{1,5}$ was zero, satisfying the phase-locking criterion.

When the respiratory period was slightly decreased to $T_{resp} = 4.48$ while keeping G to the same value of 0.2 [Fig. 2(c)], the respiration and heartbeat were still phase locked and satisfy the criterion $P_{1,5} = 1.5 \times 10^{-3} < 0.002$. However, due to the occasional jumps in the instantaneous phase, the frequency locking criterion was not satisfied any more. On

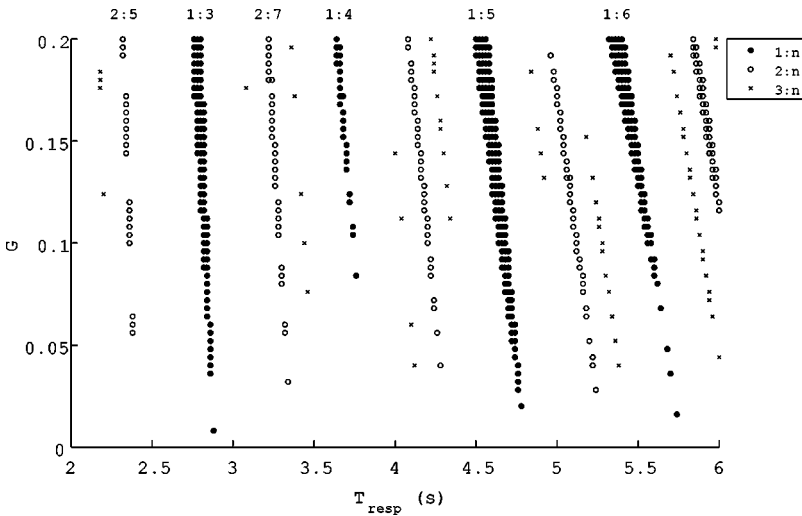


FIG. 3. Synchronized region without noise by changing parameters G (strength of the baroreflex influence on the respiratory phase) and T_{resp} (natural respiratory period). The stable synchronization was judged for each combination of G and T_{resp} with stepwise increases of 4.0×10^{-3} and 0.02 s, respectively. The region for synchronization is wider as G increases, and the width is variable depending on the ratio of synchronization.

the other hand, in case of $(G, T_{resp}) = (0.028, 4.90)$ [Fig. 2(d)], the value of $H_{1,4}$ satisfied the frequency locking criterion: indeed, for each respiratory cycle, there were always four heartbeats. However, due to the continuous phase slip, the $P_{1,4} = 0.02 > 0.002$ could not indicate the phase locking between two oscillations.

With the criteria above, we then searched for the region for the stable synchronization from a parameter space with T_{resp} ranging from 2.0 to 6.0 s (step; 0.02 s) and G ranging from 0.0 to 0.2 (step; 4.0×10^{-3}). The range of T_{resp} was chosen as typical respiratory periods in humans and that of G was set so that the respiratory phase was not reversed.

The results (Fig. 3) contain two main characteristics of the cardiorespiratory synchronization in our model. First, stable synchronization was not observed when $G = 0.0$, and the synchronized region became wider as G increased. The value $G = 0.0$ means that there is no influence of blood pressure on respiration, as in the original SH model [9]. This result implies that the baroreceptor influence on respiration, together with the respiratory influences on heartbeat, are important for this phenomenon to be observed.

Second, the width of the synchronized region depends on the ratio of synchronization. Generally, the 1:n (i.e., $m = 1$) synchronization had the wide region, and the region became narrower as m increased. Also, the region for 1:4 synchronization was much narrower than that for 1:3, and so for 1:6 synchronization as compared to 1:5.

In humans under free-running conditions, Schäfer *et al.* [4] observed many episodes of 1:3 synchronization, one of which lasted as long as 1000 s, 2:5 and 2:7 synchronizations for more than a minute, and short episodes of 1:4, 3:8, and 4:11 synchronizations. Recently, Lotrič and Stefanovska [19] also observed a 1:5 frequency locking for 200 s and a 1:7 synchronization for 70 s, although the ratio of 1:7 needs slower respiration and was out of range in our simulations.

In addition, Seidel and Herzel [7] observed a 1:4 frequency locking for 213 beats in humans under the paced breathing with the respiratory period set to 4 s, although the setting is somewhat different from ours in the sense that, with the paced breathing, momentary blood pressure fluctuations cannot modify the respiration. Further, in anesthetized

rats, Stefanovska *et al.* [20] recently reported the evolving 1:n phase lockings where n increased as the respiratory periods increased after the injection of anesthetic drug.

Thus, it can be said that our model generally captures characteristics of the cardiorespiratory synchronization in physiological settings; the robustness of 1:n compared to $m:n$ ($m = 2, 3, \dots$) ratios and the fragility of a 1:4 synchronization in humans against 1:3 and/or 1:5 synchronizations. To our knowledge, there is no other model that can explain the actual experimental results like this.

B. Synchronization with noise

It is well known that human cardiovascular variables exhibit noisy dynamics [22]. In this section, as opposed to simulations for the deterministic case above, we study how added noise affects the synchronization in our model. This strategy would also be useful in evaluating the stability of synchronization against given perturbations.

To accomplish this, we added the Gaussian white noise ξ to the baroreceptor activity v_b , of which standard deviation was set to 0.2 [Figs. 1 and 4(a)]. This magnitude of the noise was about 1/7 of the average amplitude of v_b , and roughly corresponds to the observed arterial blood pressure variability in humans [23] as compared to the pulse pressure.

Figure 4 shows examples for such simulations. When $(G, T_{resp}) = (0.2, 4.44)$, the phase stroboscope [Fig. 4(b), left] shows an acceptable 1:5 synchronization also resulting in five sharp peaks in the histogram [Fig. 4(b), right]. The indices $H_{1,5}$ and $P_{1,5}$, respectively, also satisfied the criteria for frequency and phase lockings. When $(G, T_{resp}) = (0.2, 4.40)$, however, there were many episodes of jumps and slips in the instantaneous respiratory phase [Fig. 4(c), left] and both $H_{1,5}$ and $P_{1,5}$ were not acceptable. Indeed, this phase stroboscope is much like that frequently observed in human experiments [4].

In Fig. 4(d), we also plot an index for synchronization $\lambda_{m,n}(t)$ recently proposed by Tass *et al.* [3] for noisy data. Here $\lambda_{m,n}$ is a measure of the conditional probability that the phase of one oscillator has a certain value with a small bin when the phase of another oscillator belongs to the same bin,

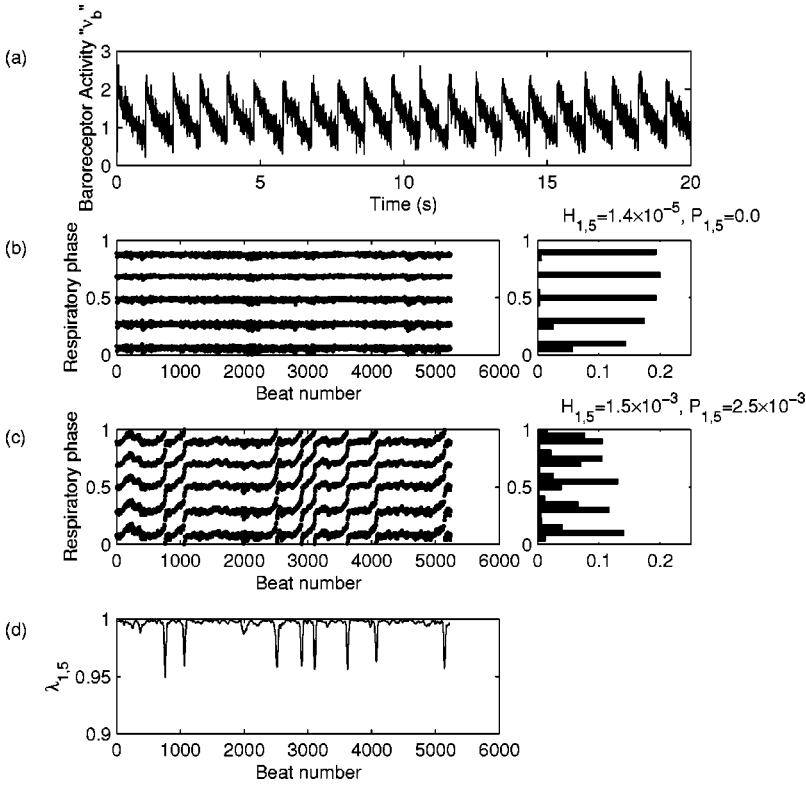


FIG. 4. Representative results of simulations with noise (the standard deviation set to 0.2) and the corresponding values for H and P . (a) Baroreceptor activity ν_b . (b) The phase stroboscope (left) and the histogram of the instantaneous respiratory phases (right) with $(G, T_{resp}) = (0.2, 4.44)$. Here H and P are small enough to be judged for the stable synchronization, although the horizontal stripes are more noisy than those without noise (Fig. 2). (c) The phase stroboscope and the histogram with $(G, T_{resp}) = (0.2, 4.40)$. Because of the noise, the synchronization is observed partially, and both H and P do not satisfy our criteria for the stable synchronization. (d) An index for synchronization $\lambda_{1,5}(t)$ [3] for the data in (c). We can see that λ detects this partially synchronized pattern.

and for completely phase-locked or completely phase-unlocked data, one respectively obtains $\lambda_{m,n} = 1.0$ or $\lambda_{m,n} = 0.0$ [3,20,21]. In our noisy simulation [Fig. 4(c)], the $\lambda_{1,5}(t)$ remained close to 1.0 for most of the time with occasional drops when big phase jumps were observed [Fig. 4(d)]. Thus, our criteria for synchronization using both $H_{m,n}$ and $P_{m,n}$ are fairly strict in that only stable synchronization behavior can be probed.

As in the preceding section, we examined the region for synchronization with noise in the same parameter space (Fig. 5). Consequently, we found that most of ratios with the smaller region in Fig. 3 disappeared and only 1: n synchronizations and a few 2:5 and 2:7 ratios remained intact. The remaining ratios were those reported to exist stably in the

original experimental demonstration by Schäfer *et al.* [4]. This again confirmed the validity of our model for cardiorespiratory synchronization in humans.

IV. MECHANISM OF SYNCHRONIZATION

In the preceding section, we showed the importance of baroreceptor influence on respiration, or G , on the cardiorespiratory synchronization in our model. Starting from this evidence, we discuss some possible mechanisms for the synchronization in the present section.

A. Effects of RSA

The original experimental demonstration of cardiorespiratory synchronization in humans [4] revealed that such syn-

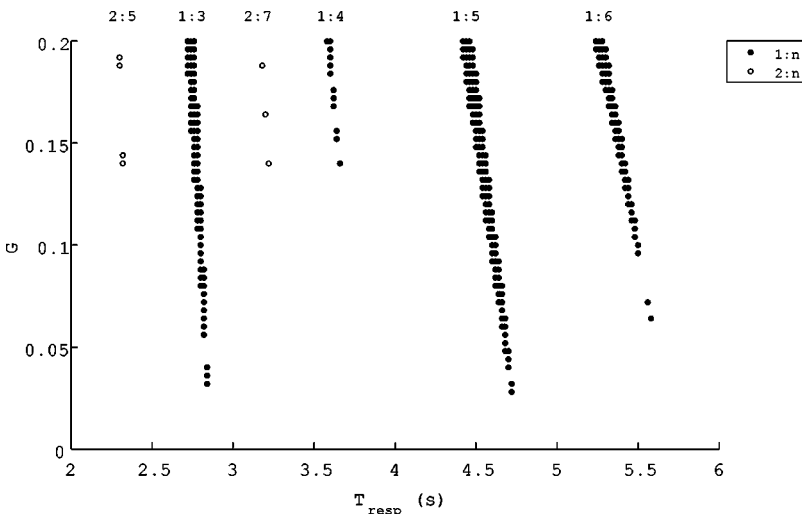


FIG. 5. Synchronized region with noise by changing parameters G (strength of the baroreflex influence on the respiratory phase) and T_{resp} (natural respiratory period). The stable synchronization was judged for each combination of G and T_{resp} with stepwise increases of 4.0×10^{-3} and 0.02 s, respectively. Simulation was performed five times and the mean H and P were used. Compared with the results without noise (Fig. 3), the region for synchronization is generally narrower and only the ratios of synchronization described by Schäfer *et al.* [4] for humans remained intact.

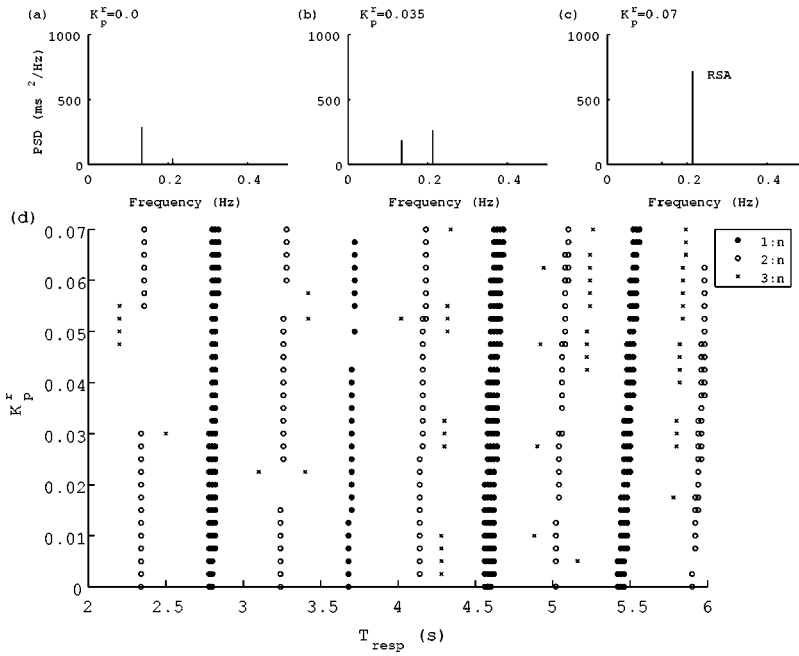


FIG. 6. (a)–(c) The effects of changing k_p^r (strength of the influence of respiration on heartbeat) on respiratory modulation of heart rate (RSA). The magnitudes of RSA are measured by the heights of power spectral peaks for cardiac interbeat intervals. (d) Synchronized region without noise by changing parameters k_p^r and T_{resp} (natural respiratory period). The stable synchronization was judged for each combination of k_p^r and T_{resp} . The G was set to a constant value of 0.14. The synchronized region is not affected by changing k_p^r .

chronization behavior was more readily observed when the magnitude of respiratory modulation of cardiac cycle length, i.e., RSA, was smaller. Recently, Lotrič and Stefanovska [19] also reported that the degree of synchronization measured by conditional probability $\lambda_{m,n}$ [3] was inversely proportional to the standard deviation of heartbeat interval time series, which is known to have moderate correlation with the magnitude of RSA. Here we study the effect of the magnitude of RSA on the synchronized region in our model.

Figure 6 shows the effects of changing k_p^r in Eq. (4) on the region for synchronization by setting G to a constant value of 0.14. The increase of k_p^r results in the greater parasympathetic modulation of heart rate, i.e., the greater RSA [Figs. 6(a–c)]. In other words, k_p^r changes the respiratory influence on heartbeat as opposed to G representing the influence of heartbeat and hence blood pressure on respiration. It was found that k_p^r does not seem to affect the synchronized region much, suggesting that the respiratory influence on heartbeat (or RSA) plays a minor role in masking the cardiorespiratory synchronization in our model.

Thus, in our model, the forced entrainment of respiration to heartbeat (and blood pressure) seems to be more important than RSA, i.e., the respiratory influence on heartbeat. An apparent contrast with the results of Schäfer *et al.* [4] and those of Lotrič and Stefanovska [19] should be explained by factors other than RSA as outlined below.

B. Effects of baroreflex sensitivity

In our model, as well as in the actual physiological system, the heartbeats are also influenced by another low-frequency oscillation, i.e., MWSA. Similar to a proposed mechanism for generation of this slow wave both in heart rate and blood pressure [24], our model generates MWSA by the delayed ($\theta_{vNe} = 4.2$ s) feedback control of blood pressure (Fig. 1) through the baroreflex control of the sympathetic efferent activity ν_s [Eq. (3)]. Thus, it would be inter-

esting to examine how the baroreflex sensitivity k_s^b could affect the synchronization behavior because this slow wave in blood pressure (Mayer wave) could affect both respiration [through Eq. (18)] and heartbeat [through Eqs. (3), (5), (6), and (7)] in different ways, and hence the greater magnitude might lead to the stronger unlocking between these two oscillators.

Figure 7 shows the results of such simulations. Increasing k_s^b resulted in the smaller magnitude of MWSA [Figs. 7(a–c)] possibly due to the reduced instability inherent to the delayed feedback system for blood pressure control. Consequently, the region for cardiorespiratory synchronization became wider as compared to that with the default value of $k_s^b = 0.7$. On the other hand, the smaller k_s^b , associated with the greater MWSA magnitude, resulted in the narrower region for synchronization.

Thus, it can be said that the sympathetic baroreflex sensitivity does affect the degree of cardiorespiratory synchronization in our model. This partly explains why Lotrič and Stefanovska [19] observed smaller $\lambda_{m,n}$ when the standard deviation of heart rate time series were greater, because the decreased k_s^b and hence the increased MWSA magnitude increase the standard deviation while the region for synchronization would be narrower. This hypothesis could easily be tested by examining the cardiorespiratory synchronization in humans and finding the difficulty in observing the synchronization behavior when the subjects are in the standing position; the MWSA is generally greater while they are standing compared to the sitting or supine position.

C. Dominance of odd ratios for synchronization

If the forced entrainment of respiration by heartbeat in “tracking” the ongoing, low-frequency fluctuations of heart rate (MWSA) and blood pressure is an important mechanism of cardiorespiratory synchronization in our model, this may in part explain the fragility of a 1:4 synchronization both in humans and in our model against 1:3 or 1:5 synchronizations.

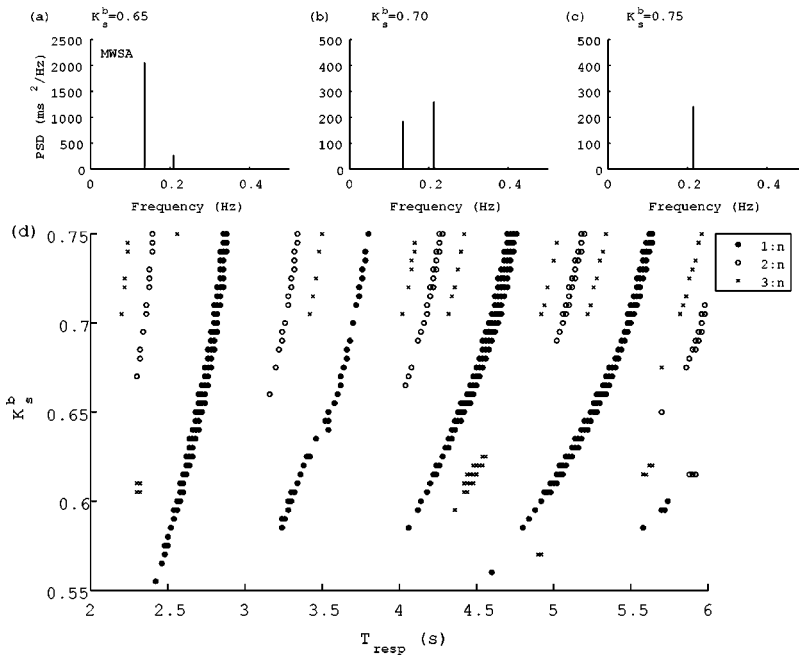


FIG. 7. (a)–(c) The effects of changing k_s^b (sympathetically mediated baroreflex sensitivity affecting the vascular dynamics) on low-frequency heart rate oscillation (MWSA). The magnitudes of MWSA are measured by the heights of power spectral peaks for cardiac inter-beat intervals. (d) Synchronized region without noise by changing parameters k_s^b and T_{resp} (natural respiratory period). The stable synchronization was judged for each combination of k_s^b and T_{resp} . The G was set to a constant value of 0.14. By decreasing the k_s^b , the region for synchronization becomes narrower.

The amount of change in respiratory periods that could be induced by Eq. (18) is roughly a function of a number of systolic parts of blood pressure wave with $v_b > v_{trig}$ within the expiratory period. When the ratio of synchronization is 1:5, for example, such numbers can range from 2 to 3, leading to the great flexibility to “adjust” respiratory periods to ongoing changes in heartbeat. When 1:4, on the other hand, this number is always 2, suggesting the loss of the flexibility to adjust respiratory periods. This may qualitatively explain why the region for 1:4 synchronization was much narrower than that for 1:3, and so was that for 1:6 synchronization as compared to 1:5 (Figs. 3 and 5). In future research, we need to develop a more quantitative formalism to account for this aspect of cardiorespiratory synchronization in humans.

V. DISCUSSION

In this paper, we investigated cardiorespiratory synchronization in humans by a structural cardiovascular model, and numerically showed that the model could exhibit the stable synchronization against given perturbations. We also showed that, in addition to a well-known influence of respiration on heartbeat, the simultaneous influence of heartbeat and hence blood pressure on respiration was important for cardiorespiratory synchronization in our model. Because cardiac influence on respiration was based on animal experiments [12,13], its existence in humans should be studied further, possibly by a method for analysis of the directionality of couplings [25], with the actual data. However, the lack of such influence in our model did not result in the stable synchronization behavior.

How can we validate our model against the actual physiological system? This is a tough question because the experimental data for this phenomenon in humans are not usually accurate enough to test the validity of our model. In further research, we might need to investigate on how each parameter would affect general pictures of the synchronization and other “complex” dynamics, and evaluate the (dis)similarity with the actual qualitative as well as quantitative dynamics in this cardiovascular and/or cardiorespiratory system.

For example, though we focused only on the stable synchronization behavior observed for the entire period of simulations, the actual human data [4] exhibit intermittent phase jumps as shown in the noisy case in Fig. 4(c) and even transitions among different locking ratios; in this sense, we only investigated in the present study the conditions under which cardiorespiratory synchronization was observed during “quiescent” phases. This intermittency and/or these transitions might introduce nonstationarity to the time series data for both heartbeat and respiration. Thus, whether our model or the variants could also simulate such intrinsic nonstationarity [26] would be of interest.

ACKNOWLEDGMENTS

We thank T. Nomura for helpful discussions and suggestions. This work was supported (to Y.Y.) by Monbusho Grant-in-Aids for Scientific Research (Grant Nos. 11694135 and 12050212). Y.A. and H.E.S. thank NIH/National Center for Research Resources (P41RR13622) and the NIA (AG14100) for partial support.

[1] S. H. Strogatz and I. Stewart, *Sci. Am.* **269**, 68 (1993).

[2] L. Glass, *Nature (London)* **410**, 277 (2001).

[3] P. Tass *et al.*, *Phys. Rev. Lett.* **81**, 3291 (1998).

[4] C. Schäfer, M. G. Rosenblum, J. Kurths, and H.-H. Abel, *Nature (London)* **392**, 239 (1998).

[5] M. G. Rosenblum *et al.*, *IEEE Eng. Med. Biol. Mag.* **17**, 46 (1998).

[6] C. Schäfer, M. G. Rosenblum, H. H. Abel, and J. Kurths, *Phys.*

- Rev. E **60**, 857 (1999).
- [7] H. Seidel and H. Herzel, IEEE Eng. Med. Biol. Mag. **17**, 54 (1998).
- [8] R. W. DeBoer, J. M. Karemaker, and J. Strackee, Am. J. Physiol. **253**, 680 (1987).
- [9] H. Seidel and H. Herzel, Physica D **115**, 145 (1998).
- [10] A. T. Winfree, J. Theor. Biol. **16**, 15 (1967).
- [11] Y. Kuramoto, *Chemical Oscillations, Waves, and Turbulence* (Springer, Berlin, 1984).
- [12] R. Jung and P. G. Katona, J. Appl. Physiol. **68**, 1465 (1990).
- [13] E. L. Dove and P. G. Katona, J. Appl. Physiol. **59**, 1258 (1985).
- [14] V. S. Reiner and C. Antzelevitch, Am. J. Physiol. **249**, H1143 (1985).
- [15] J. P. Saul, News Physiol. Sci. **5**, 32 (1990).
- [16] A. Malliani, M. Pagani, F. Lombardi, and S. Cerutti, Circulation **84**, 482 (1991).
- [17] K. Kotani, I. Hidaka, Y. Yamamoto, and S. Ozono, Methods Inf. Med. **39**, 153 (2000).
- [18] The results of spectral analysis showed that the mean heartbeat interval was 962.6 ms, the power of RSA was 263.9 ms², and that of MWSA was 246.3 ms².
- [19] M. B. Lotrić and A. Stefanovska, Physica A **283**, 451 (2000).
- [20] A. Stefanovska *et al.*, Phys. Rev. Lett. **85**, 4831 (2000).
- [21] We calculated the $\lambda_{1,n}$ as follows [20]. At the k th heartbeat at time t_k , the distribution of conditional respiratory phases $\phi_r(t_j)$ is quantified as $r_l(t_k) = [1/M_l(t_k)] \sum_{j=1}^{M_l(t_k)} e^{i\phi_r(t_j)}$ for each j , such that $t_k - t_p/2 \leq t_j < t_k + t_p/2$ when both the cardiac phases for every n beats and the respiratory phases belong to the l th ($l = 1, 2, \dots, n$) bins of each oscillator phase. Here the $M_l(t_k)$ is the number of such points at the k th instant and we set t_p to the ten times respiratory cycle. Where the phases are completely locked or completely unlocked, we obtain $|r_l(t_k)| = 1$ or $|r_l(t_k)| = 0$, respectively. To improve reliability, we calculated the average over all n bins and obtained the index of synchronization $\lambda_{1,n}(t_k) = 1/n \sum_{l=1}^n |r_l(t_k)|$.
- [22] A. L. Goldberger, D. R. Rigney, and B. J. West, Sci. Am. **262**, 42 (1990).
- [23] D. P. Veerman, B. P. M. Imholz, W. Wieling, J. M. Karemaker, and G. A. van Montfrans, Hypertension **24**, 120 (1994).
- [24] J. B. Madwed, P. Albrecht, R. G. Mark, and R. J. Cohen, Am. J. Physiol. **256**, H1753 (1989).
- [25] M. G. Rosenblum and A. S. Pikovsky, Phys. Rev. E **64**, 045202 (2001).
- [26] L. A. N. Amaral, P. Ch. Ivanov, N. Aoyagi, I. Hidaka, S. Tomono, A. L. Goldberger, H. E. Stanley, and Y. Yamamoto, Phys. Rev. Lett. **86**, 6026 (2001).